

Geometric integration of classical spin dynamics via a mean-field Schrödinger equation

David Dahlbom,¹ Hao Zhang,^{1,2} Cole Miles,³ Xiaojian Bai,⁴ Cristian D. Batista,^{1,5} and Kipton Barros^{6,*}

¹*Department of Physics and Astronomy, The University of Tennessee, Knoxville, Tennessee 37996, USA*

²*Materials Science and Technology Division, Oak Ridge National Laboratory, Oak Ridge, Tennessee 37831, USA*

³*Department of Physics, Cornell University, Ithaca, New York 14850, USA*

⁴*Neutron Scattering Division, Oak Ridge National Laboratory, Oak Ridge, TN 37831, USA*

⁵*Quantum Condensed Matter Division and Shull-Wollan Center,*

Oak Ridge National Laboratory, Oak Ridge, Tennessee 37831, USA

⁶*Theoretical Division and CNLS, Los Alamos National Laboratory, Los Alamos, New Mexico 87545, USA*

The Landau-Lifshitz equation describes the time-evolution of magnetic dipoles, and can be derived by taking the classical limit of a quantum mechanical spin Hamiltonian. To take this limit, one constrains the many-body quantum state to a tensor product of coherent states, thereby neglecting entanglement between sites. Expectation values of the quantum spin operators produce the usual classical spin dipoles. One may also consider expectation values of polynomials of the spin operators, leading to quadrupole and higher-order spin moments, which satisfy a dynamical equation of motion that generalizes the Landau-Lifshitz dynamics [Zhang and Batista, Phys. Rev. B **104**, 104409 (2021)]. Here, we reformulate the dynamics of these $N^2 - 1$ generalized spin components as a mean-field Schrödinger equation on the N -dimensional coherent state. This viewpoint suggests efficient integration methods that respect the local symplectic structure of the classical spin dynamics.

I. INTRODUCTION

The Landau-Lifshitz (LL) equation,

$$\frac{d\mathbf{s}_i}{dt} = -\mathbf{s}_i \times \frac{\partial H}{\partial \mathbf{s}_i}, \quad (1)$$

describes the time evolution of classical spins \mathbf{s}_i with conserved Hamiltonian $H(\mathbf{s}_1, \dots, \mathbf{s}_L)$. In the special case of a time-invariant effective field $\mathbf{B}_i = -\partial H/\partial \mathbf{s}_i$, each spin \mathbf{s}_i would simply precess around \mathbf{B}_i .

The LL equation is one possible classical limit of a quantum mechanical spin system. Effectively, each spin operator \hat{S}_i^α is replaced by its expectation value, $s_i^\alpha = \langle Z | \hat{S}_i^\alpha | Z \rangle$, representing the spin angular momentum on site i , measured in units of $\hbar = 1$. The quantum state is approximated as a tensor product, $|Z\rangle = |Z_1\rangle \otimes \dots \otimes |Z_L\rangle$, thereby neglecting entanglement between sites. Spin operators \hat{S}_i^α for distinct sites $i \neq j$ commute. In each local Hilbert space i , spin operators act as generators for the Lie group $SU(2)$,

$$[\hat{S}_i^\alpha, \hat{S}_i^\beta] = i \epsilon_{\alpha\beta\gamma} \hat{S}_i^\gamma, \quad (2)$$

where we use the convention of summation over repeated Greek indices (here, $\gamma = 1, 2, 3$). The fully antisymmetric Levi-Civita symbol $\epsilon_{\alpha\beta\gamma}$ appearing in this commutator is the underlying source of the vector cross product appearing in the LL dynamics. An explicit construction of the spin operators \hat{S}_i^α is presented in Appendix A.

Our interest is the study of “weakly-entangled” magnetic materials via a classical approximation that generalizes the LL dynamics [1]. This generalization is strictly

necessary to model large classes of magnets with effective spins $s > 1/2$ and strong single-ion anisotropy induced by the combination of spin-orbit coupling and crystal field effects, such as $4d - 5d$ and $4f - 5f$ -electron materials as well as several $3d$ magnets [2–4]. The generalization is also necessary to describe magnets comprising weakly-coupled entangled units, such as dimers [5], trimers [6] and tetrahedra [7].

The spin dipole \mathbf{s}_i at each site i is typically insufficient to model the state of such systems. Instead, we should incorporate all information carried by $|Z_i\rangle$, which lives in an N -dimensional local Hilbert space. That is, we should work with *coherent spin states* with respect to the fundamental representation of $SU(N)$. The local state is fully characterized by a set of $N^2 - 1$ expectation values $n_i^\alpha = \langle Z | \hat{T}_i^\alpha | Z \rangle$. The \hat{T}_i^α are generators for $SU(N)$ and satisfy

$$[\hat{T}_i^\alpha, \hat{T}_i^\beta] = i f_{\alpha\beta\gamma} \hat{T}_i^\gamma. \quad (3)$$

where $f_{\alpha\beta\gamma}$ are structure constants for the $\mathfrak{su}(N)$ Lie algebra, and the implicit sum over γ runs from 1 to $N^2 - 1$. Without loss of generality, we may take \hat{S}_i^α to be a subset of \hat{T}_i^α , such that the three components of the spin dipole s_i^α are contained within the full set of $SU(N)$ spin components n_i^α .

The generalization of LL dynamics is [1],

$$\frac{dn_i^\alpha}{dt} = f_{\alpha\beta\gamma} \frac{\partial H}{\partial n_i^\beta} n_i^\gamma, \quad (4)$$

with classical Hamiltonian $H(\mathbf{n}_1, \dots, \mathbf{n}_L)$. In the special case of $N = 2$, one recovers $f_{\alpha\beta\gamma} = \epsilon_{\alpha\beta\gamma}$ and the LL equation. Appendix B provides a derivation of this generalized spin dynamics.

This paper is concerned with the efficient numerical integration of Eq. (4), in a way that respects the underlying geometric structure. Our strategy is to reformulate

* kbarros@lanl.gov

the dynamics as a mean-field Schrödinger equation,

$$\frac{d}{dt} \mathbf{Z}_i = -i \mathfrak{H}_i \mathbf{Z}_i, \quad (5)$$

where

$$\mathfrak{H}_i = \frac{\partial H}{\partial n_i^\alpha} T^\alpha \quad (6)$$

may be interpreted as an effective local Hamiltonian that acts on the coherent state at site i . The vector $\mathbf{Z}_i \in \mathbb{C}^N$ represents components of $|Z_i\rangle$ in an arbitrary basis. Similarly, $T^\alpha \in \mathbb{C}^{N \times N}$ are matrices that describe the action of \hat{T}_i^α on states $|Z_i\rangle$. In this basis, the generalized spin components are

$$n_i^\alpha = \mathbf{Z}_i^\dagger T^\alpha \mathbf{Z}_i. \quad (7)$$

The derivation of Eq. (5) will be presented in Sec. II.

This Schrödinger viewpoint offers a powerful framework for designing numerical integration schemes. Equation (4) is known as a Lie-Poisson system, for which the Darboux-Lie theorem guarantees a local Hamiltonian structure [8, 9]. Equation (5), by contrast, introduces a canonical Hamiltonian structure that is valid *globally*. Specifically, the real and imaginary parts of the coherent state \mathbf{Z}_i act as canonical positions and momenta, which obey Hamilton's equations of motion.

Hamiltonian systems conserve a symplectic 2-form, i.e., a measure of area in phase space. Numerical integration methods that respect this symplectic structure are especially powerful, in that they enable dynamical integration over arbitrarily long time-scales without numerical drift. In Sec. III we will describe exactly symplectic integration methods for spin dynamics. Numerical benchmarks will be presented in Sec. IV.

II. CLASSICAL DYNAMICS IN THE SCHRÖDINGER PICTURE

A. Unitary evolution of expectation values

Equation (4) is a Lie-Poisson system, and describes co-adjoint orbits on the dual Lie algebra [8, 10]. We will make this statement concrete using ordinary matrix language.

Let T^α be generators for $SU(N)$ in the defining representation. That is, T^α are a basis for the Lie algebra $\mathfrak{su}(N)$, the space of traceless, Hermitian, $N \times N$ matrices. The matrix commutator is,

$$[T^\alpha, T^\beta] = i f_{\alpha\beta\gamma} T^\gamma, \quad (8)$$

inherited from that of the quantum operators, Eq. (3).

We will require that the basis satisfies an orthonormality condition,

$$\text{tr } T^\alpha T^\beta = \tau \delta_{\alpha\beta}. \quad (9)$$

This condition makes it possible to interpret T^α as a basis also for the dual Lie algebra, $\mathfrak{su}^*(N)$. Orthonormality is equivalent to antisymmetry of $f_{\alpha\beta\gamma}$ in all indices

$$f_{\alpha\beta\gamma} = -f_{\beta\alpha\gamma} = -f_{\alpha\gamma\beta}. \quad (10)$$

Our convention is to select a basis T^α that includes the three spin matrices S^α as a subset. Substitution of $T^\alpha \rightarrow S^\alpha$ into Eq. (9) determines τ , as given in Eq. (A7) of Appendix A.

Equation (4) defines the dynamics of spin components n_i^α . Equivalently, we may consider the time evolution of the matrix

$$\mathbf{n}_i = n_i^\alpha T^\alpha, \quad (11)$$

interpreted as an element of dual Lie algebra $\mathfrak{su}^*(N)$.

It will be convenient to identify the energy gradient $\partial H / \partial n_i^\alpha$ with the matrix \mathfrak{H}_i defined in Eq. (6), interpreted as an element of $\mathfrak{su}(N)$. Using this notation, Eq. (4) is compactly expressed as

$$\frac{d\mathbf{n}_i}{dt} = i [\mathbf{n}_i, \mathfrak{H}_i], \quad (12)$$

which follows from the antisymmetry of $f_{\alpha\beta\gamma}$, and the matrix commutators in Eq. (8). The dynamics may also be written

$$\mathbf{n}_i(t) = U_i(t) \mathbf{n}_i(0) U_i^{-1}(t), \quad (13)$$

where $U(t) \in \text{SU}(N)$ satisfies

$$\frac{d}{dt} U_i(t) = -i \mathfrak{H}_i(t) U_i(t), \quad (14)$$

with initial condition $U(0) = I$, as may be verified by explicit differentiation.

B. Schrödinger dynamics of coherent states

Now we will reformulate the unitary evolution of the matrix \mathbf{n}_i as a dynamics of the vector \mathbf{Z}_i that gives rise to expectation values n_i via Eq. (7). To derive this dynamics in a way that builds physical intuition, we introduce the outer product,

$$\rho_i = \mathbf{Z}_i \mathbf{Z}_i^\dagger, \quad (15)$$

in analogy with a pure density matrix for site i .

Spin components, Eq. (7), may be calculated in two different ways,

$$\text{tr } \rho_i T^\alpha = n_i^\alpha = \text{tr } \mathbf{n}_i T^\alpha / \tau. \quad (16)$$

For the second equality, we used the definition of Eq. (11) and orthonormality, Eq. (9).

The matrix ρ_i is Hermitian, and the generators T^α span all $N \times N$ Hermitian, traceless matrices. From this we deduce

$$\rho_i = \mathbf{n}_i / \tau + cI, \quad (17)$$

where I is the identity matrix, and $c = |\mathbf{Z}_i|^2/N$.

Because I commutes with any matrix, the matrices \mathbf{n}_i and ρ_i share the same dynamical equation

$$\frac{d\rho_i}{dt} = i [\rho_i, \mathfrak{H}_i]. \quad (18)$$

This dynamics may be interpreted as the von Neumann evolution of the density matrix. Equivalently,

$$\rho_i(t) = U_i(t)\rho_i(0)U_i^{-1}(t). \quad (19)$$

Referring to Eq. (15), it follows that the coherent states must evolve as,

$$\mathbf{Z}_i(t) = U_i(t)\mathbf{Z}_i(0). \quad (20)$$

Taking the time derivative of both sides, and substituting from Eq. (14) yields

$$d\mathbf{Z}_i/dt = -i\mathfrak{H}_i\mathbf{Z}_i,$$

which validates our statement that Eq. (5) is a reformulation of the generalized spin dynamics, Eq. (4).

Extending the analogy with quantum mechanics, we will refer to $\mathfrak{H}_i(t)$ as the *local Hamiltonian* on site i . In contrast, recall that $\mathfrak{H}_i(t)$ was defined in Eq. (6) as the embedding of the classical Hamiltonian gradient $\partial H/\partial n_i^\alpha$ into the Lie algebra $\mathfrak{su}(N)$. To understand how these two viewpoints are compatible, we refer to Appendix B. For the generalized spin dynamics in the fundamental representation of $SU(N)$, the classical Hamiltonian H of Eq. (B8) is obtained from the many-body quantum Hamiltonian \hat{H} under the substitution $\hat{T}_i^\alpha \rightarrow n_i^\alpha$. Furthermore, the spin components n_i^α for each site i appear at most linearly in each term of H . Then \mathfrak{H}_i may be viewed as a semiclassical approximation to \hat{H} , in which we make the substitution $\hat{T}_j^\alpha \rightarrow n_j^\alpha$ only for sites $j \neq i$.

The results of this section may be restated in a more abstract and general mathematical language. Equation (12) can be viewed as an isospectral flow $dW/dt = [B, W]$, with $W = \mathbf{n}_i$ and $B = (i\mathfrak{H}_i)^\dagger$. The eigenvalues of W are constants of motion. Each eigenvector \mathbf{v} of W satisfies the dynamical equation $d\mathbf{v}/dt = B\mathbf{v}$, corresponding to our Schrödinger equation. Although we derived this result in the context of the Lie-Poisson system on $\mathfrak{su}(N)$, it generalizes to a much broader class of so-called *reductive* Lie algebras [11, 12]. Note that most classical Lie algebras are reductive, including $\mathfrak{gl}(N, \mathbb{C})$, $\mathfrak{gl}(N, \mathbb{R})$, $\mathfrak{so}(N)$, and $\mathfrak{sp}(N)$, in addition to our working example of $\mathfrak{su}(N)$. In our application to spin dynamics, we benefit from the fact that a single eigenvector, $\mathbf{v} = \mathbf{Z}_i$, fully describes the matrix $W = \mathbf{n}_i$. More generally, if the initial condition $W(0)$ has low rank (up to some constant shift), then the time-evolved state $W(t)$ will continue to have low rank, and modeling the dynamics through the time-evolving eigenvectors becomes beneficial.

C. Conservation laws

Lie-Poisson systems such as Eq. (4) satisfy a number of conservation laws. Some of these are associated with the

geometric structure of the phase space, and are independent of the choice of Hamiltonian. One may verify that any function $C(\mathbf{n}_i)$ that satisfies $(\partial C/\partial n_i^\alpha) f_{\alpha\beta\gamma} n_i^\gamma = 0$ is a constant of motion. Such functions arise from Casimirs of the Lie algebra, i.e., symmetric, homogeneous polynomials of the basis matrices T^α that commute with all algebra elements. There are $N - 1$ Casimirs of $SU(N)$. The simplest example is the quadratic Casimir $\sum_\alpha (n_i^\alpha)^2$ which, for spin- $\frac{1}{2}$ systems, reduces to the dipole magnitude squared.

A second class of conservation laws arise from symmetries of the Hamiltonian. For example, energy is a constant of motion provided that the Hamiltonian has no explicit time-dependence. One may verify $dH/dt = 0$ directly by contracting $\partial H/\partial n_i^\alpha$ on both sides of Eq. (4), and using the antisymmetry of $f_{\alpha\beta\gamma}$.

The Schrödinger dynamics, Eq. (5), is equivalent to the generalized spin dynamics, Eq. (4), and therefore shares these conservation laws.

Equation (4) has the form of a Lie-Poisson system. The Darboux-Lie theorem states that Lie-Poisson systems have a local Hamiltonian structure [8, 9]. That is, in the neighborhood of each spin configuration n_i^α , there exists a change of coordinates that gives rise to canonical variables $(\mathbf{p}_i, \mathbf{q}_i)$ that satisfy Hamilton's equations of motion locally. Interestingly, the Schrödinger equation gives rise to a Hamiltonian dynamics that is valid *globally*. Specifically, in Appendix C we demonstrate that the real and imaginary components of the coherent state,

$$\mathbf{Z}_i = (\mathbf{p}_i - i\mathbf{q}_i)/\sqrt{2}, \quad (21)$$

satisfy Hamilton's equations of motion,

$$\frac{d\mathbf{p}_i}{dt} = -\frac{\partial H}{\partial \mathbf{q}_i}, \quad \frac{d\mathbf{q}_i}{dt} = +\frac{\partial H}{\partial \mathbf{p}_i}. \quad (22)$$

The canonical Hamiltonian structure of the Schrödinger equation ensures conservation of the symplectic 2-form $\sum_{i,a} dp_{i,a} \wedge dq_{i,a}$.

D. State normalization

The magnitude of \mathbf{Z}_i is a conserved quantity in the Schrödinger dynamics, Eq. (5). Absent other knowledge, the normalization convention $|\mathbf{Z}_i| = 1$ is a natural choice, and emphasizes the interpretation of \mathbf{Z}_i as a quantum mechanical coherent spin state. Rescaling \mathbf{Z}_i can be useful, however, to adjust the overall magnitude of the classical spin components. A carefully selected rescaling can strongly enhance the agreement between an approximate classical model and the true quantum mechanical system [13].

Consider, first, the LL dynamics of spin dipoles, Eq. (1). This coincides with Eq. (4) on the Lie algebra $\mathfrak{su}(N = 2)$, such that the matrices T^α appearing in Eq. (6) are the three generators S^α of $SU(2)$. Although

we have so far interpreted T^α as generators in the fundamental representation of $SU(N)$, this assumption is unnecessary. In particular, we can faithfully describe the LL equation using generators T^α in any irreducible representation of $SU(2)$, labeled by spin $s \in \{\frac{1}{2}, 1, \frac{3}{2}, \dots\}$. Each dipole magnitude $|\mathbf{s}_i|$ is a conserved quantity of the LL dynamics, and takes the value $s|\mathbf{Z}_i|^2$ in the spin- s representation. To model a LL dynamics with dipole magnitude $|\mathbf{s}_i| = s_0$, we should normalize \mathbf{Z}_i such that

$$|\mathbf{Z}_i|^2 = s_0/s \quad (23)$$

Consider, second, the generalized spin dynamics, Eq. (4), interpreted as the unitary evolution of coherent spin states \mathbf{Z}_i in the fundamental representation of $SU(N)$. Equivalently, we may model the dynamics of the $N^2 - 1$ spin components n_i^α under the $SU(N)$ group action. Here, $|\mathbf{n}_i| = s|\mathbf{Z}_i|^2$, where $s = (N-1)/2$. One may wish to select the normalization of \mathbf{Z}_i according to a quantum mechanical sum rule derived from the $SU(N)$ quadratic Casimir.

III. NUMERICAL METHODS

Geometric integration aims to approximate the flow of a dynamical system while exactly satisfying geometrical constraints [9, 14, 15]. For example, Eq. (19) suggests that one integration time-step should take the form [10]

$$\rho_i(t) \rightarrow \rho_i(t + \Delta t) = U_t \rho_i(t) U_t^{-1}. \quad (24)$$

To obtain an exactly unitary matrix U_t that approximates the integral of Eq. (14), one may use, e.g., the method of Runge-Kutta Munthe-Kaas [16]. This unitary evolution ensures conservation of Casimirs, but conservation of other geometrical properties, such as the local symplectic 2-form, is not automatically guaranteed.

Designing efficient symplectic integration schemes for Lie-Poisson systems is a topic of considerable interest [17–20]. A common strategy is to employ operator splitting and the fact that the composition of symplectic maps is again symplectic. For example, in the context of the LL equation, one may partition the spins into non-interacting groups, and cycle through symplectic updates for each of these groups using symmetric Strang splitting (i.e., a Suzuki-Trotter type decomposition) [21–23].

Alternatively, one may seek symplectic integrators for Lie-Poisson systems that update all dynamical variables simultaneously, and in a symmetric way. The spherical midpoint method, designed specifically for the LL equation, is one example [24]. Quite recently, Modin and Viviani introduced the class of Isospectral Symplectic Runge–Kutta methods (IsoSyRK) [11], which applies to any Lie-Poisson system on a reductive Lie algebra; this covers most Lie-Poisson systems of practical interest, including generalized spin dynamics on $\mathfrak{su}(N)$, and the LL equation as a special case. The Isospectral Minimal Midpoint (IMM) method is a particularly elegant variant of IsoSyRK [12].

The standard implicit midpoint method is known to be symplectic when applied to canonical Hamiltonian systems [9]. We will next demonstrate that the implicit midpoint method applied to the Schrödinger equation (5) coincides with IMM method applied to the equivalent Lie-Poisson system, Eq. (4).

A. Schrödinger midpoint

To integrate Eq. (5) over one time-step $\mathbf{Z}_i \rightarrow \mathbf{Z}'_i$, the implicit midpoint method has the symmetric form

$$\frac{\mathbf{Z}'_i - \mathbf{Z}_i}{\Delta t} = -i \tilde{\mathfrak{H}}_i \tilde{\mathbf{Z}}_i, \quad (25)$$

The right-hand side involves the midpoint state,

$$\tilde{\mathbf{Z}}_i = \frac{\mathbf{Z}'_i + \mathbf{Z}_i}{2}. \quad (26)$$

The symbol $\tilde{\mathfrak{H}}_i$ denotes the local Hamiltonian of Eq. (6), evaluated as a function of $\tilde{\mathbf{Z}}_j$ at all sites j .

The self-consistent value of \mathbf{Z}'_i may be calculated numerically as follows. Starting with an initial guess $\mathbf{Z}'_{i,0} = \mathbf{Z}_i$, we iteratively calculate

$$\tilde{\mathbf{Z}}_{i;k} = \frac{1}{2} (\mathbf{Z}'_{i;k} + \mathbf{Z}_i), \quad (27)$$

$$\mathbf{Z}'_{i;k+1} = \mathbf{Z}_i - i \Delta t \tilde{\mathfrak{H}}_{i;k} \tilde{\mathbf{Z}}_{i;k}, \quad (28)$$

with $\tilde{\mathfrak{H}}_{i;k}$ defined in the natural way. Iterations terminate when $\mathbf{Z}'_{i;k}$ has converged within numerical tolerance. For example, at 64-bit floating point precision, we may require $|\mathbf{Z}'_{i;k+1} - \mathbf{Z}'_{i;k}| < 10^{-14}$. This condition is typically satisfied in $k \lesssim 10$ iterations, given a reasonably small step size Δt .

The Schrödinger equation is a canonical Hamiltonian system, via Eqs. (21) and (22). For such systems, the implicit midpoint method is known to be a symplectic integrator [9].

The Schrödinger midpoint method is norm preserving. To see this, we left-multiply both sides of Eq. (25) by $\tilde{\mathbf{Z}}_i^\dagger$,

$$\frac{1}{2\Delta t} (\mathbf{Z}'_i + \mathbf{Z}_i)^\dagger (\mathbf{Z}'_i - \mathbf{Z}_i) = -i \tilde{\mathbf{Z}}_i^\dagger \tilde{\mathfrak{H}}_i \tilde{\mathbf{Z}}_i. \quad (29)$$

The right-hand side is purely imaginary, since $\tilde{\mathfrak{H}}_i$ is Hermitian. Setting the real terms on the left-hand side to zero, we find $|\mathbf{Z}_i|^2 = |\mathbf{Z}'_i|^2$.

We will now demonstrate that the Schrödinger midpoint method is an instance of the IMM method [11, 12]. The density matrix $\rho_i = \mathbf{Z}_i \mathbf{Z}_i^\dagger$ evolves according to Eq. (18). This dynamics can be understood as an isospectral flow $dW/dt = [B(W), W]$ where $B = -i \tilde{\mathfrak{H}}_i$ and $W = \rho_i$. One time-step $W \rightarrow W'$ of the IMM method is defined as,

$$W = \left(I - \frac{\Delta t}{2} B(\tilde{W}) \right) \tilde{W} \left(I + \frac{\Delta t}{2} B(\tilde{W}) \right) \quad (30)$$

$$W' = \left(I + \frac{\Delta t}{2} B(\tilde{W}) \right) \tilde{W} \left(I - \frac{\Delta t}{2} B(\tilde{W}) \right). \quad (31)$$

where the midpoint state \tilde{W} and final state W' are to be solved self-consistently.

Equations (25) and (26) may be rewritten as

$$\mathbf{Z}_i = \left(I + i \frac{\Delta t}{2} \tilde{\mathfrak{H}}_i \right) \tilde{\mathbf{Z}}_i \quad (32)$$

$$\mathbf{Z}'_i = \left(I - i \frac{\Delta t}{2} \tilde{\mathfrak{H}}_i \right) \tilde{\mathbf{Z}}_i. \quad (33)$$

Intuitively, this says that the midpoint state $\tilde{\mathbf{Z}}_i$ can be obtained either by integrating forward from \mathbf{Z}_i , or backward from \mathbf{Z}'_i . Calculating the outer products $W = \mathbf{Z}_i \mathbf{Z}_i^\dagger$ and $W' = \mathbf{Z}'_i \mathbf{Z}'_i^\dagger$, we exactly reproduce the IMM equations. Note that Eq. (26) defines $\tilde{\mathbf{Z}}_i$ as a simple vector average of the initial and final states, whereas $\tilde{W} = \tilde{\mathbf{Z}}_i \tilde{\mathbf{Z}}_i^\dagger$ cannot be expressed that way.

B. Schrödinger midpoint applied to the LL equation

The LL dynamics, Eq. (1), is a special case of the generalized spin dynamics, Eq. (4). It can therefore be formulated as a Schrödinger equation on an $SU(2)$ representation, and integrated using the midpoint method, Eqs. (25) and (26). In the special cases of spin- $\frac{1}{2}$ and spin-1 representations, the Schrödinger midpoint method may be equivalently reformulated as an update rule operating directly on spin dipoles, $\mathbf{s}_i \rightarrow \mathbf{s}'_i$. The final result, derived in Appendix D, is

$$\mathbf{s}_i = \tilde{\mathbf{s}}_i + \frac{\Delta t}{2} \tilde{\mathbf{s}}_i \times \frac{\partial H}{\partial \tilde{\mathbf{s}}_i} - \frac{\Delta t^2}{4} f(\tilde{\mathbf{s}}_i) \quad (34)$$

$$\mathbf{s}'_i = \tilde{\mathbf{s}}_i - \frac{\Delta t}{2} \tilde{\mathbf{s}}_i \times \frac{\partial H}{\partial \tilde{\mathbf{s}}_i} - \frac{\Delta t^2}{4} f(\tilde{\mathbf{s}}_i), \quad (35)$$

where the quadratic correction,

$$f(\tilde{\mathbf{s}}_i) = \begin{cases} \frac{1}{2} \frac{\partial H}{\partial \tilde{\mathbf{s}}_i} \left(\frac{\partial H}{\partial \tilde{\mathbf{s}}_i} \cdot \tilde{\mathbf{s}}_i \right) - \frac{1}{4} \left| \frac{\partial H}{\partial \tilde{\mathbf{s}}_i} \right|^2 \tilde{\mathbf{s}}_i & (\text{spin-}\frac{1}{2}) \\ \frac{\partial H}{\partial \tilde{\mathbf{s}}_i} \left(\frac{\partial H}{\partial \tilde{\mathbf{s}}_i} \cdot \tilde{\mathbf{s}}_i \right) & (\text{spin-1}) \end{cases}, \quad (36)$$

depends on the representation. The midpoint state $\tilde{\mathbf{s}}_i$ may be solved self-consistently from the initial state \mathbf{s}_i using Eq. (34). We emphasize that $\tilde{\mathbf{s}}_i$ is *not* a simple average of \mathbf{s}_i and \mathbf{s}'_i . Once $\tilde{\mathbf{s}}_i$ is known, the final state \mathbf{s}'_i may be solved directly using Eq. (35).

The spin- $\frac{1}{2}$ variant of the Schrödinger dynamics coincides with the methodological framework presented in Ref. 25, albeit in a different language. In our notation, the expected dipole is $s^\alpha = \mathbf{Z}_i^\dagger \sigma^\alpha \mathbf{Z}_i / 2$, where σ^α are the Pauli spin matrices. In the math literature, this functional dependence $\mathbf{s}_i(\mathbf{Z}_i)$ is known as the *momentum map* [8]. The functional dependence $H(\mathbf{Z}_i)$ is called the *collective Hamiltonian*.

The spin-1 variant of Eqs. (34) and (35) was previously derived in Ref. 12 by applying the IMM method to the Lie-Poisson system on $\mathfrak{so}(3)$. Recall that the generators of $SO(3)$ in its defining representation are also generators of $SU(2)$ in its spin-1 representation.

C. Spherical midpoint

The spherical midpoint method is a powerful symplectic integrator for the LL equation [24]. One integration time-step $\mathbf{s} \rightarrow \mathbf{s}'$ is defined by the update rule

$$\frac{\mathbf{s}'_i - \mathbf{s}_i}{\Delta t} = -\bar{\mathbf{s}}_i \times \frac{\partial H}{\partial \bar{\mathbf{s}}_i}, \quad (37)$$

involving the normalized midpoint dipole,

$$\bar{\mathbf{s}}_i = \frac{\mathbf{s}'_i + \mathbf{s}_i}{|\mathbf{s}'_i + \mathbf{s}_i|}. \quad (38)$$

The classical Hamiltonian on the right-hand side $H(\bar{\mathbf{s}}_1, \dots, \bar{\mathbf{s}}_L)$ is evaluated at the midpoint spin configuration.

The new spin \mathbf{s}' can be solved self-consistently using iterations analogous to Eqs. (27) and (28). Here, however, normalization of the midpoint spin $\bar{\mathbf{s}}$ is employed, which is crucial to the good properties of the method. Different proofs of the symplectic structure have been given [26].

D. Heun-projected (HeunP)

All methods above are symplectic. For purposes of benchmarking, we will also compare with the Heun method, a non-symplectic Runge-Kutta scheme of second order. Applied to Eq. (5), one full integration time-step is

$$\mathbf{Z}_i^{(1)} = \mathbf{Z}_i - i \Delta t \tilde{\mathfrak{H}}_i \mathbf{Z}_i \quad (39)$$

$$\mathbf{Z}_i^{(2)} = \mathbf{Z}_i - \frac{i \Delta t}{2} \left(\tilde{\mathfrak{H}}_i \mathbf{Z}_i + \tilde{\mathfrak{H}}_i^{(1)} \mathbf{Z}_i^{(1)} \right), \quad (40)$$

$$\mathbf{Z}'_i = \mathbf{Z}_i^{(2)} / |\mathbf{Z}_i^{(2)}|. \quad (41)$$

The first step can be interpreted as an explicit Euler predictor for the update. The second, corrector step involves the local Hamiltonian $\tilde{\mathfrak{H}}_i^{(1)}$ evaluated at $\mathbf{Z}_j^{(1)}$ for all j . Finally, the output \mathbf{Z}'_i is normalized using a projection step. We use the name HeunP in reference to prior work that employed the same scheme to integrate the stochastic LL equation [27, 28].

IV. NUMERICAL BENCHMARKS

A. Model definitions

For our numerical examples, we consider the 1D Heisenberg spin chain with an easy-axis anisotropy. We start from the quantum Hamiltonian,

$$\hat{\mathcal{H}} = J \sum_{i=1}^L \hat{\mathbf{S}}_i \cdot \hat{\mathbf{S}}_{i+1} + D \sum_{i=1}^L (\hat{S}_i^z)^2, \quad (42)$$

where \hat{S}^α denote spin operators in the spin-1 representation. We will study this model in two classical limits.

The LL dynamics, Eq. (1), retains only the spin dipole degrees of freedom. Its classical Hamiltonian

$$H^{\text{LL}} = J \sum_{i=1}^L \mathbf{s}_i \cdot \mathbf{s}_{i+1} + D \sum_{i=1}^L (s_i^z)^2, \quad (43)$$

is obtained from $\hat{\mathcal{H}}$ under the substitution rule $\hat{\mathbf{s}}_i \rightarrow \mathbf{s}_i$. We will employ the normalization convention $|\mathbf{s}_i| = 1$. The LL dynamics can be formulated as a Schrödinger dynamics in some spin- s representation of SU(2). Per Eq. (23), the proper normalization of states is $|\mathbf{Z}_i|^2 = 1/s$.

The generalized spin dynamics (GSD) of Eq. (4) describes an alternative classical limit. This approach retains more features from the quantum mechanical dynamics, and enables modeling of the single-ion anisotropy in a more physically correct way. Polynomials of local spin-1 operators \hat{S}^α act on kets $|Z_i\rangle$, viewed as coherent states in the fundamental representation of SU(3). Each spin dipole \mathbf{s}_i generalizes to an eight component vector \mathbf{n}_i that includes the original dipole \mathbf{s}_i , as well as five additional quadrupole components. The SU(3) spin \mathbf{n}_i carries information equivalent to the local coherent state $|Z_i\rangle$.

The GSD classical Hamiltonian is defined as the expected energy,

$$H^{\text{GSD}} = \langle Z | \hat{\mathcal{H}} | Z \rangle, \quad (44)$$

where $|Z\rangle$ is constrained to be a tensor product state over the local coherent spin states. Following the arguments of Appendix B, the result is

$$H^{\text{GSD}} = J \sum_{i=1}^L \mathbf{s}_i \cdot \mathbf{s}_{i+1} + D \sum_{i=1}^L c_\alpha n_i^\alpha, \quad (45)$$

up to an irrelevant constant shift. We have used the expansion,

$$(S^z)^2 = c_0 I + c_\alpha T^\alpha. \quad (46)$$

where the spin-1 matrices S^α are a subset of the generators T^α of SU(3) in the defining representation. Although we picked an easy-axis anisotropy, any single-ion anisotropy term could be expanded in this manner. The coefficients c_α may be calculated explicitly using Eq. (9), but doing so is not needed for the numerics.

Substitution of H^{GSD} into Eq. (4) defines the generalized spin dynamics. In practice, we will employ the Schrödinger formulation, Eq. (5). Inserting $\partial H^{\text{GSD}} / \partial n_i^\alpha$ into Eq. (6), we find the local Hamiltonian to be

$$\mathfrak{H}_i^{\text{GSD}} = J(s_{i-1}^\alpha + s_{i+1}^\alpha)S^\alpha + Dc_\alpha T^\alpha. \quad (47)$$

In a numerical implementation, it may be convenient to now undo the expansion of Eq. (46),

$$\mathfrak{H}_i^{\text{GSD}} = J(s_{i-1}^\alpha + s_{i+1}^\alpha)S^\alpha + D[(S^z)^2 - c_0 I]. \quad (48)$$

Equations (5) and (48), with $s_i^\alpha = \mathbf{Z}_i^\dagger S^\alpha \mathbf{Z}_i$, are closed. In this context, we take $|\mathbf{Z}_i|^2 = 1$. We need not explicitly select the full set of SU(3) generators T^α . A valid set of spin-1 matrices S^α is given in Eq. (A2).

The c_0 term in (48) ensures $\text{tr } \mathfrak{H}_i^{\text{GSD}} = 0$. For the true Schrödinger equation, this constant shift has the effect of rescaling \mathbf{Z}_i by a physically irrelevant pure phase. For numerical integration schemes, however, this constant shift may meaningfully affect the approximation.

B. Dynamics of a single ion

As a first test, we will consider the dynamics of a single ion, setting $J = 0$. The anisotropy strength, D , can be absorbed into an overall rescaling of time. We consider a purely dipole initial condition,

$$\mathbf{s}(t=0) = \begin{bmatrix} s_0^x \\ s_0^y \\ s_0^z \end{bmatrix} = \begin{bmatrix} \sin(\theta) \\ 0 \\ \cos(\theta) \end{bmatrix} \quad (49)$$

where θ denotes the polar angle relative to the z -axis.

For the case of the LL dynamics, the time-evolution is a simple precession about the z -axis,

$$\mathbf{s}^{\text{LL}}(t) = \begin{bmatrix} s_0^x \cos(\omega^{\text{LL}} t) \\ s_0^x \sin(\omega^{\text{LL}} t) \\ s_0^z \end{bmatrix}, \quad (50)$$

where $\omega^{\text{LL}} = 2Ds_0^z$ is the angular frequency of precession.

For the case of the GSD on an SU(3) spin, the general trajectory for an arbitrary initial condition is given in Ref. 1. For our pure dipole initial condition, the dipole part of the trajectory is

$$\mathbf{s}^{\text{GSD}}(t) = \begin{bmatrix} s_0^x \cos(\omega^{\text{GSD}} t) \\ s_0^x s_0^z \sin(\omega^{\text{GSD}} t) \\ s_0^z \end{bmatrix}. \quad (51)$$

Observe that this dynamics is still described by a precession about the z -axis. Now, however, the precession frequency $\omega^{\text{GSD}} = D$ is independent of the initial angle θ . Furthermore, the y -component of spin is reduced by the factor s_0^z , such that the total spin dipole magnitude is no longer a constant of motion. A reduction in $|\mathbf{s}(t)|^2$ indicates that weight has been transferred to the quadrupole part of the full SU(3) spin $\mathbf{n}(t)$. Recall that the quadratic Casimir, $|\mathbf{n}(t)|^2$, is a constant of motion.

Figure 1 illustrates the numerical integration of the LL and GSD trajectories using the Schrödinger midpoint method for spin- $\frac{1}{2}$ and spin-1 respectively, and $\theta = 2\pi/5$. A fairly large integration time-step $\Delta t = 0.5$ was selected to emphasize numerical error. For the LL dynamics, we also tried the spherical midpoint method, and observed errors to be about 2 times smaller. For both LL and GSD cases, energy conservation appears to be numerically exact under the Schrödinger midpoint integration scheme.

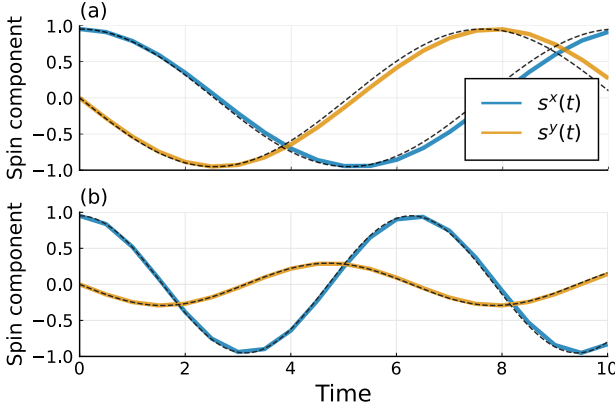


Figure 1. Trajectories of x and y spin dipole components for a single-ion Hamiltonian with an easy-axis anisotropy, $D = -1$. Numerical integration uses a large time step, $\Delta t = 0.5$, to emphasize error. (a) LL dynamics using the Schrödinger midpoint method in the spin- $\frac{1}{2}$ representation. (b) Generalized spin dynamics using the Schrödinger midpoint method in the spin-1 representation, which describes SU(3) spins. Dashed black lines indicate reference trajectories given in Eqs. (50) and Eq. (51).

C. Dynamics of a spin chain

Next, we study a chain of $L = 100$ spins with periodic boundary conditions, and a ferromagnetic Heisenberg interaction $J = -1$. We follow Ref. 12 and select an initial state consisting of smoothly varying pure spin dipoles,

$$\mathbf{s}_i = \begin{bmatrix} \cos(2\pi x_i^2) \sin(2\pi x_i^3) \\ \sin(2\pi x_i^2) \sin(2\pi x_i^3) \\ \cos(2\pi x_i^3) \end{bmatrix} \quad (52)$$

where $x_i = (i - 1)/99$ for indices $i = 1 \dots 100$.

1. LL dynamics of a pure Heisenberg chain

In the absence of the anisotropy term, $D = 0$, the classical Hamiltonian is purely a function of the spin dipole, and the LL and GSD coincide.

Figure 2 illustrates the approximate conservation of energy for the various integration schemes applicable. Note that the Schrödinger midpoint method and the spherical midpoint method are both symplectic, and therefore do not exhibit significant energy drift over large time-scales. In contrast, the HeunP scheme is non-symplectic, and does not prevent drift in energy. In this example, all symplectic integration schemes demonstrate remarkable conservation of energy. As we will show in the next example, setting $D \neq 0$ significantly reduces the accuracy of energy conservation. Finally, we remark that the Schrödinger midpoint result with spin-1 precisely reproduces the curve shown in the top panel of Fig. 4 in Ref. 12. To reproduce the bottom panel of Fig. 4 in Ref. 12, we

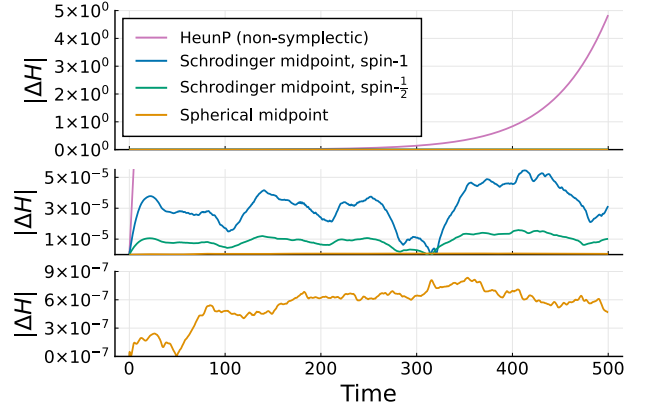


Figure 2. Energy fluctuations $\Delta H = H(t) - H(0)$ for the numerically integrated LL dynamics of a pure Heisenberg spin chain, $J = -1$, absent anisotropy, $D = 0$. We compare the following integration methods: the HeunP method applied to the Schrödinger equation, the Schrödinger midpoint method in the spin- $\frac{1}{2}$ and spin-1 representations, and the spherical midpoint method. The integration time-step is $\Delta t = 0.1$. The same data is plotted on three different energy scales to illustrate the huge variation between the integration schemes for this model.

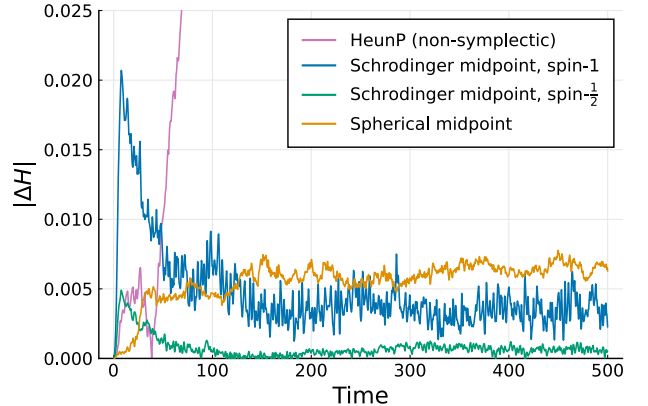


Figure 3. Energy fluctuations for the numerically integrated LL dynamics of a Heisenberg spin chain with $J = -1$, now including an easy-axis anisotropy, $D = -1$. The numerical integration schemes are the same as in Fig. 2, but here we use a much smaller integration time-step, $\Delta t = 0.02$.

needed to integrate the spherical midpoint method backwards in time.

2. LL dynamics including easy-axis anisotropy

We now include an easy-axis anisotropy, $D = -1$, in the Heisenberg chain. With this additional term, the LL and GSD classical limits deviate. Here we will consider the LL dynamics.

Figure 3 compares accuracy of the four integration schemes. Relative to Fig. 2, we observe much larger en-

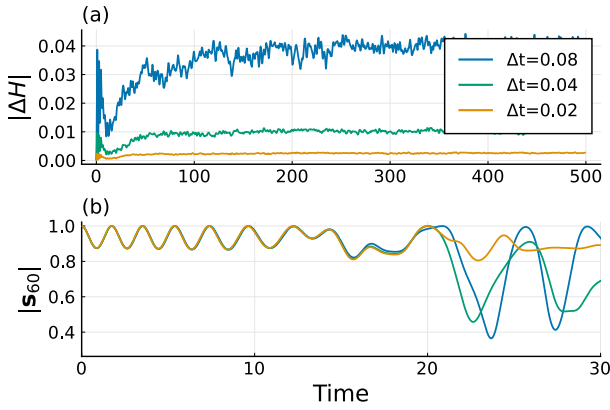


Figure 4. (a) Energy fluctuations for the numerically integrated GSD of a Heisenberg spin chain with $J = -1$ and easy-axis anisotropy, $D = -1$, in the spin-1 representation. We use the Schrödinger midpoint method with varying time-step Δt . (b) Time evolution of the dipole magnitude $|\mathbf{s}_i|$ for site index $i = 60$.

ergy fluctuations, despite a significantly smaller time-step of $\Delta t = 0.02$ (down from $\Delta t = 0.1$). Energy fluctuations observed from the Schrödinger midpoint and spherical midpoint numerical integration schemes are now of the same order. In all cases tested, when applying the Schrödinger midpoint to the LL dynamics, the spin- $\frac{1}{2}$ representation is preferred over the spin-1 representation. There remains a tremendous advantage in using a symplectic integration scheme—the energy of the HeunP method continues to drift strongly.

3. GSD including easy-axis anisotropy

Our final numerical benchmark is the Heisenberg spin chain with easy-axis anisotropy $D = -1$ using the generalized spin dynamics. Here we must work in the spin-1 representation, i.e. using $SU(3)$ spins, for which the traditional LL numerical integration schemes do not apply.

Figure 4 shows time integration using the Schrödinger midpoint method. The top panel illustrates that the energy fluctuations decrease approximately quadratically with time-step Δt , consistent with the second order accuracy of the implicit midpoint method [9]. The bottom panel shows the time evolution of the dipole magnitude $|\mathbf{s}_i|$ for site index $i = 60$. Fluctuations in the dipole magnitude are possible because weight can be transferred to the quadrupole part of the $SU(3)$ spins \mathbf{n}_i . All spins in the initial configuration, Eq. (52), are pure dipoles, with a relatively slow variation along the spin chain. Therefore the initial dynamics is reasonably well approximated by the single ion limit, $J \approx 0$, previously considered in Fig. 1. At times $t \gtrsim 10$, however, high-frequency spatial variations in the spin chain propagate to site $i = 60$. At

this point, chaotic dynamics can be observed, and the three trajectories integrated using different Δt quickly separate. As expected for a symplectic integrator, no significant energy drift is observed over arbitrarily long trajectory lengths.

V. CONCLUSIONS

We have presented a numerical integration scheme, the Schrödinger midpoint method, that applies to the generalized dynamics of $SU(N)$ spins, Eq. (4). In the special case of the Landau-Lifshitz dynamics, Eq. (1), this method reduces to previously known symplectic integrators [12, 25]. The Schrödinger midpoint method can be viewed as a special case of the Isospectral Midpoint Method [11, 12], which applies to general Lie-Poisson systems. As applied to the generalized spin dynamics, our approach has the numerical advantage of describing the evolution of a vector (the coherent spin state) rather than that of a full matrix. The method exactly respects the local symplectic structure of the Lie-Poisson system, or equivalently, the *global* symplectic structure of the Schrödinger equation, which may be understood as a canonical Hamiltonian system. We anticipate that this method will be of broad applicability to the study of spin $s > \frac{1}{2}$ systems with strong single-ion anisotropy, for which the spin quadrupole (and perhaps higher-order) moments cannot be ignored [1, 4, 29–32].

ACKNOWLEDGMENTS

We thank Martin Mourigal and Ying Wai Li for insightful discussions. This work was supported by the U.S. Department of Energy, Office of Science, Office of Basic Energy Sciences, under Award No. DE-SC0022311.

Appendix A: Spin operators as representations of $SU(2)$

Here we review some properties of the irreducible representations of $SU(2)$, which serve as quantum spin operators. The $SU(2)$ irreps are conventionally labeled by a spin index $s \in \{\frac{1}{2}, 1, \frac{3}{2}, \dots\}$, and have dimension $N = 2s + 1$.

For spin $1/2$, a conventional basis for the spin matrices is

$$S^x = \frac{1}{2} \begin{bmatrix} 0 & 1 \\ 1 & 0 \end{bmatrix}, \quad S^y = \frac{1}{2} \begin{bmatrix} 0 & -i \\ i & 0 \end{bmatrix}, \quad S^z = \frac{1}{2} \begin{bmatrix} 1 & 0 \\ 0 & -1 \end{bmatrix}. \quad (A1)$$

In other words, $S^\alpha = \sigma^\alpha/2$, where σ^α are the Pauli matrices.

For spin 1, we could define

$$S^x = \frac{1}{\sqrt{2}} \begin{bmatrix} 0 & 1 & 0 \\ 1 & 0 & 1 \\ 0 & 1 & 0 \end{bmatrix}, S^y = \frac{1}{\sqrt{2}} \begin{bmatrix} 0 & -i & 0 \\ i & 0 & -i \\ 0 & i & 0 \end{bmatrix}, S^z = \begin{bmatrix} 1 & 0 & 0 \\ 0 & 0 & 0 \\ 0 & 0 & -1 \end{bmatrix}. \quad (\text{A2})$$

This pattern generalizes to arbitrary spin s ,

$$S^x = \begin{bmatrix} 0 & a_1 & & & \\ a_1 & 0 & \ddots & & \\ & \ddots & \ddots & a_{N-1} & \\ & & a_{N-1} & 0 & \end{bmatrix}, S^y = \begin{bmatrix} 0 & -ia_1 & & & \\ ia_1 & 0 & \ddots & & \\ & \ddots & \ddots & -ia_{N-1} & \\ & & ia_{N-1} & 0 & \end{bmatrix}, S^z = \begin{bmatrix} s & & & & \\ & s-1 & & & \\ & & \ddots & & \\ & & & -s & \end{bmatrix}, \quad (\text{A3})$$

where $N = 2s + 1$, and the off diagonal elements, $a_j = \frac{1}{2} \sqrt{2(s+1)j - j(j+1)}$, satisfy the symmetry $a_j = a_{N-j}$.

The spin matrices S^α define the action of the quantum spin operators. The many-body spin operator \hat{S}_i^α is defined to act only on the i th local Hilbert space,

$$\hat{S}_i^\alpha = \underbrace{I \otimes \cdots \otimes \hat{S}^\alpha}_{\text{ith term}} \otimes \cdots \otimes I.$$

The local operator \hat{S}^α is defined by its action $\langle e_a | \hat{S}^\alpha | e_b \rangle = (S^\alpha)_{ab}$ in some basis $|e_1\rangle, \dots, |e_N\rangle$. The operators \hat{S}_i^α share all mathematical properties of the matrices S^α , to be listed below.

By construction, the spin matrices satisfy the commutation relations,

$$[S^\alpha, S^\beta] = i \epsilon_{\alpha\beta\gamma} S^\gamma, \quad (\text{A4})$$

which gives rise to the same commutation relations, Eq. (2), for the quantum spin operators.

The N eigenvalues for each spin matrix S^α run from $m = -s, \dots, s$. The total angular momentum for each spin i is scalar, i.e.,

$$|\mathbf{S}|^2 = (S^x)^2 + (S^y)^2 + (S^z)^2 = s(s+1)I, \quad (\text{A5})$$

with I the identity matrix. This polynomial is the sole Casimir of $\mathfrak{su}(2)$.

The spin matrices satisfy the orthonormality condition

$$\text{tr } S^\alpha S^\beta = \tau \delta_{\alpha\beta}, \quad (\text{A6})$$

which is a special case of Eq. (9). The normalization constant is the sum of squares of eigenvalues,

$$\tau = \sum_{m=-s}^s m^2 = \frac{2}{3}s \left(s + \frac{1}{2} \right) (s+1). \quad (\text{A7})$$

Appendix B: Review of generalized spin dynamics

Following Ref. 1, we here review how Eq. (4) emerges as a classical limit of a many-body quantum system.

Consider a many-body quantum spin Hamiltonian $\hat{\mathcal{H}}$, such as the spin chain model of Eq. (42). This Hamiltonian may involve spin operators \hat{S}^α with spin representation s , corresponding to local Hilbert space dimension $N = 2s + 1$. The choice $s > 1/2$ would be appropriate to model, e.g., the effective spin angular momentum associated with a collection of spins that have aligned according to Hund's rules.

For $N > 2$, the Hamiltonian may include local anisotropy terms, such as $(\hat{S}_i^z)^2$. Such terms are *not* a linear combination of the \hat{S}_i^α , i.e., do not generate usual rotations of the local spin state. Importantly, however, any local physical operator *can* be decomposed as a linear combination of the $(N^2 - 1)$ generators \hat{T}_i^α of $\text{SU}(N)$ in the fundamental representation, plus a constant shift.

Using the completeness of the generators \hat{T}_i^α in each local Hilbert space, we can write a general Hamiltonian as a polynomial expansion,

$$\hat{\mathcal{H}} = \sum_i J_{(i,\alpha)}^{(1)} \hat{T}_i^\alpha + \frac{1}{2} \sum_{i,j} J_{(i,\alpha),(j,\beta)}^{(2)} \hat{T}_i^\alpha \hat{T}_j^\beta + \dots, \quad (\text{B1})$$

up to an irrelevant constant shift. Recall that summation over repeated Greek indices is implied.

Any coefficient $J_{[\dots]}^{(n)}$ that couples a site with itself (e.g., a single-ion anisotropy term) can be effectively absorbed into lower order coefficients $J_{[\dots]}^{(n-1)}$ by the completeness of the generators \hat{T}_i^α for each site i . Therefore, without loss of generality, we require that the coefficients couple only distinct sites, e.g.,

$$J_{(i,\alpha),(j,\beta)}^{(2)} \propto (1 - \delta_{ij}). \quad (\text{B2})$$

Since \hat{T}_i^α and \hat{T}_j^β commute for $i \neq j$, we also have freedom to symmetrize the coefficients, e.g.,

$$J_{(i,\alpha),(j,\beta)}^{(2)} = J_{(j,\beta),(i,\alpha)}^{(2)}. \quad (\text{B3})$$

The Hamiltonian $\hat{\mathcal{H}}$ determines the evolution of a general quantum state,

$$\frac{d}{dt}|\psi\rangle = e^{-i t \hat{\mathcal{H}}} |\psi\rangle, \quad (\text{B4})$$

where we take $\hbar = 1$. The time evolution of an arbitrary expectation value $\langle \hat{A} \rangle = \langle \psi | \hat{A} | \psi \rangle$ follows,

$$i \frac{d}{dt} \langle \hat{A} \rangle = \langle [\hat{A}, \hat{\mathcal{H}}] \rangle. \quad (\text{B5})$$

To take the classical limit, we will ignore quantum entanglement and approximate the time-evolving many-body state $|\psi\rangle$ as a tensor product of coherent states of a given algebra,

$$|\psi\rangle \approx |Z\rangle = \bigotimes_{i=1}^L |Z_i\rangle. \quad (\text{B6})$$

In the remainder of this section, our purpose is to demonstrate the following: *This approximation yields a self-consistent and closed dynamics on local expectation values*, namely, Eq. (4).

Product states allow the factorization of expectation values over distinct sites,

$$\langle Z | \hat{T}_i^\alpha \hat{T}_j^\beta | Z \rangle = n_i^\alpha n_j^\beta. \quad (\text{B7})$$

It follows that, under the assumption of Eq. (B6), the expected energy $H = \langle \hat{\mathcal{H}} \rangle$ is

$$H = \sum_i J_{(i,\alpha)}^{(1)} n_i^\alpha + \frac{1}{2} \sum_{i,j} J_{(i,\alpha),(j,\beta)}^{(2)} n_i^\alpha n_j^\beta + \dots \quad (\text{B8})$$

In other words, substituting $\hat{T}_i^\alpha \rightarrow n_i^\alpha$ in the quantum Hamiltonian $\hat{\mathcal{H}}$ yields the classical Hamiltonian H .

Inserting the general Hamiltonian of Eq. (B1) into the dynamics Eq. (B5) for a local operator $\hat{A} = \hat{A}_k$ yields,

$$\begin{aligned} i \frac{d}{dt} \langle \hat{A}_k \rangle &= \sum_i J_{(i,\alpha)}^{(1)} \langle [\hat{A}_k, \hat{T}_i^\alpha] \rangle \\ &\quad + \frac{1}{2} \sum_{i,j} J_{(i,\alpha),(j,\beta)}^{(2)} \langle [\hat{A}_k, \hat{T}_i^\alpha \hat{T}_j^\beta] \rangle + \dots \end{aligned} \quad (\text{B9})$$

For the first term, we use

$$\sum_i J_{(i,\alpha)}^{(1)} [\hat{A}_k, \hat{T}_i^\alpha] = J_{(k,\alpha)}^{(1)} [\hat{A}_k, \hat{T}_k^\alpha]. \quad (\text{B10})$$

For the second term, Eq. (B2) ensures $i \neq j$, and we require either $k = i$ or $k = j$. It follows,

$$\begin{aligned} \frac{1}{2} \sum_{i,j} J_{(i,\alpha),(j,\beta)}^{(2)} [\hat{A}_k, \hat{T}_i^\alpha \hat{T}_j^\beta] &= \frac{1}{2} [\hat{A}_k, \hat{T}_k^\alpha] \sum_j \left(J_{(k,\alpha),(j,\beta)}^{(2)} \hat{T}_j^\beta + J_{(j,\alpha),(k,\beta)}^{(2)} \hat{T}_j^\alpha \right) \\ &= [\hat{A}_k, \hat{T}_k^\alpha] \sum_j J_{(k,\alpha),(j,\beta)}^{(2)} \hat{T}_j^\beta. \end{aligned} \quad (\text{B11})$$

In the second step, we used the symmetrization convention of Eq. (B3). Combining results, and using again the approximation Eq. (B6) to factorize the expectation values on distinct sites, we find

$$i \frac{d}{dt} \langle \hat{A}_k \rangle = \langle [\hat{A}_k, \hat{T}_k^\alpha] \rangle \left(J_{(k,\alpha)}^{(1)} + \sum_j J_{(k,\alpha),(j,\beta)}^{(2)} \langle \hat{T}_j^\beta \rangle + \dots \right). \quad (\text{B12})$$

The second factor on the right-hand side is $\partial H / \partial n_k^\alpha$, and this result holds to all expansion orders. Relabeling $(k, \alpha) \rightarrow (i, \beta)$, the result is

$$i \frac{d}{dt} \langle \hat{A}_i \rangle = \langle [\hat{A}_i, \hat{T}_i^\beta] \rangle \frac{\partial H}{\partial n_i^\beta}, \quad (\text{B13})$$

which is valid for any local operator \hat{A}_i . Selecting $\hat{A}_i = \hat{T}_i^\alpha$ and using Eq. (3), we reproduce the generalized spin dynamics, Eq. (4),

$$\frac{d}{dt} n_i^\alpha = f_{\alpha,\beta,\gamma} \frac{\partial H}{\partial n_i^\beta} n_i^\gamma. \quad (\text{B14})$$

Although we motivated the form of $\hat{\mathcal{H}}$ in Eq. (B1) using the language of spin systems, this Hamiltonian is in fact fully general. We could have taken each local Hilbert space i to represent, e.g., a tensor product space of *multiple* quantum spins. The time evolution of classical expectation values, Eq. (B14), would then capture quantum entanglement effects within each local Hilbert space.

Appendix C: Hamiltonian structure of the Schrödinger equation

Each $\mathfrak{su}(N)$ generator can be decomposed into its purely real and imaginary parts,

$$T^\alpha = A^\alpha + i B^\alpha. \quad (\text{C1})$$

Because T^α is Hermitian, it follows that A^α and B^α are symmetric and antisymmetric, respectively.

Substituting this decomposition into the Schrödinger equation of Eq. (5), we find

$$\frac{d}{dt} \mathbf{Z}_i = \frac{\partial H}{\partial n_i^\alpha} (-i A^\alpha + B^\alpha) \mathbf{Z}_i. \quad (\text{C2})$$

Decomposing the state vector into real and imaginary parts,

$$\mathbf{Z}_i = \frac{1}{\sqrt{2}} (\mathbf{p}_i - i \mathbf{q}_i), \quad (\text{C3})$$

allows formulation of the Schrödinger equation as an entirely real dynamics,

$$\frac{d\mathbf{p}_i}{dt} = \frac{\partial H}{\partial n_i^\alpha} (-A^\alpha \mathbf{q}_i + B^\alpha \mathbf{p}_i) \quad (\text{C4})$$

$$\frac{d\mathbf{q}_i}{dt} = \frac{\partial H}{\partial n_i^\alpha} (A^\alpha \mathbf{p}_i + B^\alpha \mathbf{q}_i). \quad (\text{C5})$$

Expectation values $n_i^\alpha = \mathbf{Z}_i^\dagger T^\alpha \mathbf{Z}_i$ may be written,

$$n_i^\alpha = \frac{1}{2} (\mathbf{p}_i - i \mathbf{q}_i)^\dagger T^\alpha (\mathbf{p}_i - i \mathbf{q}_i). \quad (\text{C6})$$

Expanding the right-hand side, and decomposing T^α into its symmetric and antisymmetric parts, we find

$$\begin{aligned} n_i^\alpha &= \frac{1}{2} \mathbf{p}_i^T A^\alpha \mathbf{p}_i + \frac{1}{2} \mathbf{q}_i^T A^\alpha \mathbf{q}_i \\ &\quad - \frac{1}{2} \mathbf{q}_i^T B^\alpha \mathbf{p}_i + \frac{1}{2} \mathbf{p}_i^T B^\alpha \mathbf{q}_i. \end{aligned} \quad (\text{C7})$$

Differentiation yields

$$\frac{\partial n_i^\alpha}{\partial \mathbf{p}_i} = A^\alpha \mathbf{p}_i + B^\alpha \mathbf{q}_i \quad (\text{C8})$$

$$\frac{\partial n_i^\alpha}{\partial \mathbf{q}_i} = A^\alpha \mathbf{q}_i - B^\alpha \mathbf{p}_i. \quad (\text{C9})$$

Energy derivatives can now be evaluated. Using the chain rule,

$$\frac{\partial H}{\partial \mathbf{p}_i} = \frac{\partial H}{\partial n_i^\alpha} (A^\alpha \mathbf{p}_i + B^\alpha \mathbf{q}_i) \quad (\text{C10})$$

$$\frac{\partial H}{\partial \mathbf{q}_i} = \frac{\partial H}{\partial n_i^\alpha} (A^\alpha \mathbf{q}_i - B^\alpha \mathbf{p}_i). \quad (\text{C11})$$

Inserting these results into Eqs. (C4) and (C5), we find that the Schrödinger equation is described by Hamilton's equations of motion,

$$\frac{d\mathbf{p}_i}{dt} = -\frac{\partial H}{\partial \mathbf{q}_i}, \quad \frac{d\mathbf{q}_i}{dt} = +\frac{\partial H}{\partial \mathbf{p}_i}. \quad (\text{C12})$$

Appendix D: Derivation of the Schrödinger midpoint formulas for LL dynamics

In this Appendix, we derive the results stated in Sec. III B. The LL dynamics of spin dipoles, Eq. (1), may be formulated as a Schrödinger dynamics, Eq. (5), involving generators S^α of $\text{SU}(2)$ in some representation. The midpoint method applied to the Schrödinger dynamics can be interpreted as two half time-steps, Eq. (32)

and (33). Consider the former, from which we determine

$$s_i^\alpha = \tilde{\mathbf{Z}}_i^\dagger \left(S^\alpha + i \frac{\Delta t}{2} [S^\alpha, \tilde{\mathbf{H}}_i] - \frac{\Delta t^2}{4} \tilde{\mathbf{H}}_i S^\alpha \tilde{\mathbf{H}}_i \right) \tilde{\mathbf{Z}}_i, \quad (\text{D1})$$

where $s_i^\alpha = \mathbf{Z}_i^\dagger S^\alpha \mathbf{Z}_i$.

For the first term, we use $\tilde{s}^\alpha = \tilde{\mathbf{Z}}_i^\dagger S^\alpha \tilde{\mathbf{Z}}_i$.

The second term may be expanded using Eq. (6),

$$i [S^\alpha, \tilde{\mathbf{H}}] = i \frac{\partial H}{\partial \tilde{s}_i^\beta} [S_\alpha, S_\beta]. \quad (\text{D2})$$

Employing the Lie bracket of Eq. (A4), we find in vector notation,

$$i [\mathbf{S}, \tilde{\mathbf{H}}] = \mathbf{S} \times \frac{\partial H}{\partial \tilde{s}_i} \quad (\text{D3})$$

To evaluate the third term, we must incorporate more information about the matrix representation of the generators S^α . Let us introduce the concise notation,

$$\tilde{\mathbf{H}}_i = \frac{\partial H}{\partial \tilde{s}_i^\beta} S^\beta = \mathbf{a} \cdot \mathbf{S} \quad (\text{D4})$$

$$S^\alpha = \mathbf{b} \cdot \mathbf{S}. \quad (\text{D5})$$

In the special cases of the spin- $\frac{1}{2}$ and spin-1 representations, the matrix spin operators satisfy

$$(\mathbf{a} \cdot \mathbf{S})(\mathbf{b} \cdot \mathbf{S})(\mathbf{a} \cdot \mathbf{S}) = \begin{cases} \frac{(\mathbf{a} \cdot \mathbf{b})(\mathbf{a} \cdot \mathbf{S})}{2} - \frac{|\mathbf{a}|^2(\mathbf{b} \cdot \mathbf{S})}{4} & (\text{spin-}\frac{1}{2}) \\ (\mathbf{a} \cdot \mathbf{b})(\mathbf{a} \cdot \mathbf{S}) & (\text{spin-1}) \end{cases}, \quad (\text{D6})$$

which are in fact valid for arbitrary $\mathbf{a}, \mathbf{b} \in \mathbb{C}^3$.

It follows,

$$\tilde{\mathbf{H}} \mathbf{S} \tilde{\mathbf{H}} = \begin{cases} \frac{1}{2} \frac{\partial H}{\partial \tilde{s}_i} \left(\frac{\partial H}{\partial \tilde{s}_i} \cdot \mathbf{S} \right) - \frac{1}{4} \left| \frac{\partial H}{\partial \tilde{s}_i} \right|^2 \mathbf{S} & (\text{spin-}\frac{1}{2}) \\ \frac{\partial H}{\partial \tilde{s}_i} \left(\frac{\partial H}{\partial \tilde{s}_i} \cdot \mathbf{S} \right). & (\text{spin-1}) \end{cases} \quad (\text{D7})$$

Inserting these results into Eq. (D1) yields Eq. (34). Similarly, we can derive Eq. (35) by starting from Eq. (33). Combined, these equations provide a closed-form update rule entirely in terms of the spin dipoles.

[1] H. Zhang and C. D. Batista, Phys. Rev. B **104**, 104409 (2021).
[2] V. S. Zapf, D. Zocco, B. R. Hansen, M. Jaime, N. Harrison, C. D. Batista, M. Kenzelmann, C. Niedermayer, A. Lacerda, and A. Paduan-Filho, Phys. Rev. Lett. **96**, 077204 (2006).
[3] S.-H. Do, H. Zhang, T. J. Williams, T. Hong, V. O. Garlea, J. Rodriguez-Rivera, T.-H. Jang, S.-W. Cheong, J.-H. Park, C. D. Batista, *et al.*, Nature communications **12**, 1 (2021).
[4] X. Bai, S.-S. Zhang, Z. Dun, H. Zhang, Q. Huang, H. Zhou, M. B. Stone, A. I. Kolesnikov, F. Ye, C. D. Batista, and M. Mourigal, Nat. Phys. **17**, 467 (2021).
[5] M. Jaime, V. F. Correa, N. Harrison, C. D. Batista, N. Kawashima, Y. Kazuma, G. A. Jorge, R. Stern, I. Heinmaa, S. A. Zvyagin, Y. Sasago, and K. Uchinokura, Phys. Rev. Lett. **93**, 087203 (2004).
[6] Y. Qiu, C. Broholm, S. Ishiwata, M. Azuma, M. Takano, R. Bewley, and W. J. L. Buyers, Phys. Rev. B **71**, 214439 (2005).
[7] Y. Okamoto, G. J. Nilsen, J. P. Attfield, and Z. Hiroi, Phys. Rev. Lett. **110**, 097203 (2013).

[8] J. E. Marsden and T. S. Ratiu, *Introduction to Mechanics and Symmetry, A Basic Exposition of Classical Mechanical Systems*, Texts in Applied Mathematics, Vol. 17 (Springer Berlin Heidelberg, 1999).

[9] E. Hairer, C. Lubich, and G. Wanner, *Geometric Numerical Integration: Structure-Preserving Algorithms for Ordinary Differential Equations*, Springer Series in Computational Mathematics, Vol. 31 (Springer Berlin Heidelberg, 2006).

[10] K. Engø and S. Faltinsen, SIAM J. Numer. Anal. **39**, 128 (2001).

[11] K. Modin and M. Viviani, Found Comput Math **20**, 889 (2020).

[12] M. Viviani, Bit Numer Math **60**, 741 (2020).

[13] T. Huberman, D. A. Tennant, R. A. Cowley, R. Coldea, and C. D. Frost, Journal of Statistical Mechanics: Theory and Experiment

[14] A. Iserles, H. Z. Munthe-Kaas, S. P. Nørsett, and A. Zanna, Acta Numerica **9**, 215 (2000).

[15] A. Iserles and G. R. W. Quispel, arXiv:1602.07755 [math] (2016), arXiv:1602.07755 [math].

[16] H. Munthe-Kaas, Bit Numer Math **38**, 92 (1998).

[17] G. Zhong and J. E. Marsden, Physics Letters A **133**, 134 (1988).

[18] P. J. Channell and J. C. Scovel, Physica D: Nonlinear Phenomena **50**, 80 (1991).

[19] R. I. McLachlan, Phys. Rev. Lett. **71**, 3043 (1993).

[20] R. I. McLachlan and C. Scovel, J Nonlinear Sci **5**, 233 (1995).

[21] M. Krech, A. Bunker, and D. P. Landau, Computer Physics Communications **111**, 1 (1998).

[22] I. P. Omelyan, I. M. Mryglod, and R. Folk, Phys. Rev. Lett. **86**, 898 (2001).

[23] J. Tranchida, S. J. Plimpton, P. Thibaudeau, and A. P. Thompson, Journal of Computational Physics **372**, 406 (2018).

[24] R. I. McLachlan, K. Modin, and O. Verdier, Phys. Rev. E **89**, 061301 (2014).

[25] R. I. McLachlan, K. Modin, and O. Verdier, IMA Journal of Numerical Analysis **35**, 546 (2015).

[26] R. McLachlan, K. Modin, and O. Verdier, Math. Comp. **86**, 2325 (2017).

[27] B. Skubic, J. Hellsvik, L. Nordström, and O. Eriksson, J. Phys.: Condens. Matter **20**, 315203 (2008).

[28] J. H. Mentink, M. V. Tretyakov, A. Fa **2008**, R05017 (2008). I. Katsnelson, and T. Rasing, J. Phys.: Condens. Matter **22**, 176001 (2010).

[29] Y. Akagi, Y. Amari, N. Sawado, and Y. Shnir, Phys. Rev. D **103**, 065008 (2021), arXiv:2101.10566.

[30] K. Remund, R. Pohle, Y. Akagi, J. Romhányi, and N. Shannon, arXiv:2203.09819 [cond-mat] (2022), arXiv:2203.09819 [cond-mat].

[31] Y. Amari, Y. Akagi, S. B. Gudnason, M. Nitta, and Y. Shnir, arXiv:2204.01476 [cond-mat, physics:hep-th] (2022), arXiv:2204.01476 [cond-mat, physics:hep-th].

[32] H. Zhang, Z. Wang, D. Dahlbom, K. Barros, and C. D. Batista, arXiv:2203.15248 [cond-mat] (2022), arXiv:2203.15248 [cond-mat].